

LEAST-MEAN-SQUARE WEIGHTED PARALLEL IIR FILTERS IN ACTIVE-NOISE-CONTROL HEADPHONES

Markus Guldenschuh

Institute of Electronic Music and Acoustics
University of Music and Performing Arts Graz
Inffeldgasse 10/3, 8010 Graz, Austria

ABSTRACT

Adaptive filters in noise control applications have to approximate the primary path and compensate for the secondary-path. This work shows that the primary- and secondary-path variations of noise control headphones depend above all on the direction of incident noise and the tightness of the ear-cups. Both kind of variations are investigated by preliminary measurements, and it is further shown that the measured variations can be approximated with the linear combination of only a few prototype filters. Thus, a parallel adaptive linear combiner is suggested instead of the typical adaptive transversal-filter. Theoretical considerations and experimental results reveal that the parallel structure performs equally well, converges even faster, and requires fewer adaptation weights.

Index Terms— Adaptive linear combiner, adaptive filter, noise control headphones

1. INTRODUCTION

Active-Noise-Control (ANC) headphones cancel incident ambient noise by playing back a destructively interfering 'anti-noise'. In adaptive feedforward ANC-headphones as in Fig. 1, a reference x of the ambient noise is sensed with a microphone outside the headphone (M_{ref}). The noise propagates through the primary path $P(j\omega)$ (i.e. the earcup), and, at the same time, the reference x is fed through the adaptive filter g and is played back via the secondary-path $S(j\omega)$ (i.e. the loudspeaker) as 'anti-noise' y . Inside the ear-cups, the residual noise e is sensed with an error microphone M_e and is fed back to the adaptation algorithm. A very popular adaptation algorithm is the Least Mean Square (LMS) because it is easy to implement and cost-efficient [1]. For systems with non-negligible secondary-paths, x is filtered with a secondary-path model \hat{S} in order to keep the reference time-aligned with the error signal; a strategy that is called filtered-x-LMS (fxLMS) algorithm.

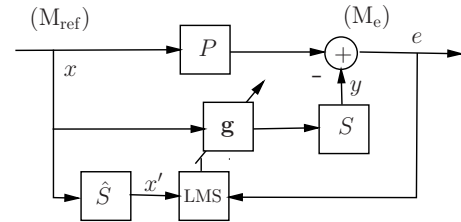


Fig. 1. Adaptive noise control: Due to the delay in the secondary path S , the input to the LMS update has to be filtered with a model of \hat{S} , too, which results in the filtered-x-LMS.

The adaptive filter itself is mostly an FIR filter. IIR filters would need fewer coefficients to yield similar transfer-functions, but adapting the poles of IIRs might lead to instabilities [2]. Therefore it has been suggested to keep the poles fixed and to adapt only the zeros [3–5], or at least find some FIR basis function that are able to model the poles [6]. The pole locations are determined by preliminary offline measurements of the system.

In the case of ANC headphones, the primary path $P(j\omega)$ and the secondary-path $S(j\omega)$ (as in Fig. 1) have to be measured for different directions of incident sound and different fittings of the headphones. Since not only the pole but also the zero locations are readily known from such measurements, this work proposes to determine the relevant zero-pole combinations via a principal component analysis (PCA) and to implement the resulting IIR filters in parallel as adaptive linear combiner (ALC) like in Fig. 2. Its output is the linear combination $\mathbf{g}^T \mathbf{H}^T \mathbf{x}$, where \mathbf{x} is a vector of input samples, \mathbf{g} is the vector of the adaptive weights and the columns of \mathbf{H} hold the impulse responses of the filters H_i .

The performance of the parallel IIR filters is compared with an adaptive transversal-filter. The parallel IIRs yield the same minimum-mean-square-error at a faster convergence and with a minimal adaptation effort.

This work has been supported in part by the K-Project ASD. The project is funded in the context of COMET - Competence Centres for Excellent Technologies - by the Austrian government.

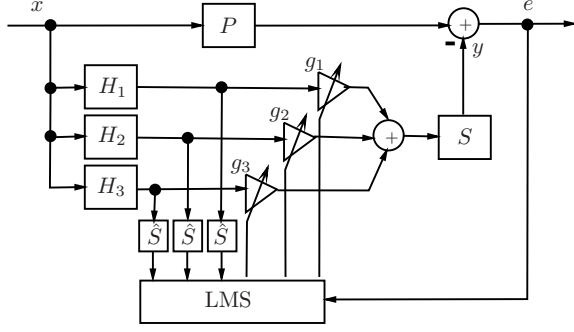


Fig. 2. Adaptive linear combiner with three parallel filters H_i

2. REVIEW OF THE LMS ADAPTATION

The functionality and properties of ANC and the LMS are well described in. [1, 7]. Its update reads as

$$\mathbf{g}[n+1] = \mathbf{g}[n] + \mu e[n] \mathbf{x}'[n], \quad (1)$$

where \mathbf{g} is a vector of FIR filter taps (cf. Fig. 1) or a vector of output weights of the adaptive linear combiner (cf. Fig. 2), respectively; and \mathbf{x}' is a vector of filtered input samples.

In case of the transversal filter of Fig. 1, the input samples \mathbf{x} are convolved with an estimate \hat{s} of the secondary-path impulse response $\mathbf{x}' = \hat{s}[n] * \mathbf{x}$. In the case of the parallel adaptive combiner of Fig. 2, \mathbf{x} is additionally filtered with the parallel filters $H_l(j\omega)$ yielding $\mathbf{x}' = \hat{s}[n] * \mathbf{H}^T \mathbf{x}$.

For the following text, it is important to review the step size μ and the speed of convergence. The optimum choice for μ depends on the eigenvalues of the input autocorrelation matrix $\mathbf{R} = \mathbf{X}'^T \mathbf{X}'$, where \mathbf{X}' is a convolution matrix of the filtered reference inputs

$$\mathbf{X}' = \begin{bmatrix} x'_{[n]} & x'_{[n-1]} & \cdots & x'_{[n-L+1]} \\ x'_{[n+1]} & x'_{[n]} & \ddots & x'_{[n-L+2]} \\ \vdots & \ddots & \ddots & \vdots \\ x'_{[n+N-1]} & x'_{[n+N-2]} & \cdots & x'_{[n+N-L]} \end{bmatrix}, \quad (2)$$

with L corresponding to the length of vector \mathbf{g} and N is the length of the analysis window for the autocorrelation.

It is shown in [1, 7] that the LMS converges if $0 < \mu < \frac{1}{\lambda_{\max}}$ and it converges fastest if $\mu = \frac{1}{2\lambda_{\max}}$, where λ_{\max} is the largest eigenvalue of \mathbf{R} . The convergence time is bounded by the ratio between the largest and the smallest eigenvalue, i.e. the condition number of \mathbf{R} .

3. PLANT VARIATIONS

The optimum adaptive transversal filter \mathbf{g}_{opt} of Fig. 1 has to approximate the primary path $P(j\omega)$ and compensate for the secondary-path $S(j\omega)$. In the frequency domain, it therefore reads as $G_{\text{opt}}(j\omega) = \frac{P(j\omega)}{S(j\omega)}$. It is advantageous to have

an adaptive filter because both paths, $P(j\omega)$ and $S(j\omega)$ may change during the usage of the ANC headphones.

- The primary path $P(j\omega)$ is the sound pressure relation between the internal microphone (at point M_e) and the external microphone (M_{ref}). Firstly, this pressure relation depends on the passive attenuation of the ear-cups and therefore on the tightness of the wearing situation. Secondly, the phase of $P(j\omega)$ depends on the direction of incident sound.
- The secondary-path $S(j\omega)$ is the transfer-function from the loudspeaker to the error microphone inside the ear-cup. This transfer-function again depends on the tightness of the headphones. In the tight case, the ear-cup is like a pressure chamber that allows reproducing enough low frequency sound pressure level to get a flat frequency response of $S(j\omega)$. In the leaky case, the low frequency sound is diffracted to the outside of the ear-cups and therefore the soundpower inside the headphones is diminished [8].

It has to be assumed that the direction of incident sound changes permanently while wearing ANC headphones because noise sources (e.g. traffic noise) move and users turn their heads. Moreover, changes in the tightness of the headphones may occur if the headphones are shifted or slightly lifted, especially in the case of non-circumaural headphones.

3.1. Plant Measurements

We measured $P(j\omega)$ and $S(j\omega)$ for all these main potential variations. The headphones were put on a mannequin which was placed on a turntable in the centre of a circular vertical loudspeaker array as in Fig. 3. $P(j\omega)$ was measured with sine sweeps for 168 different directions for tight and leaky positioned headphones resulting in $L = 336$ measurements. For the latter, the headphones were shifted back such that a leak of approximately 2 mm in diameter was provoked between the ear-cups and the intertragic notch of the mannequin's ear. The secondary path $S(j\omega)$ was measured by playing back the sine sweep via the headphones and the results are shown in Fig. 4. As mentioned earlier, a magnitude drop-off can be observed at low frequencies if the headphones are worn in a leaky manner.

Fig. 5 shows the standard deviation of $P(j\omega)$ over all measured variations. Between 200 Hz and 1000 Hz neither the magnitude nor the phase varies a lot. In this frequency band a single static filter could yield robust ANC, too. However, for the frequencies below 200 Hz and above 1000 Hz, an adaptive filter is required to cover all the variations.

Since we already know (the main) required filter variations, we do not need a fully adaptive filter. The question is much more: Is there a set of filters $H_i(j\omega)$ that can model all $l = 1 \dots L$ transfer-functions $W_l(j\omega) = \frac{P_l(j\omega)}{S_l(j\omega)}$ in the form of the ALC in Fig. 2. This question can be answered by means of a Principal Component Analysis (PCA).

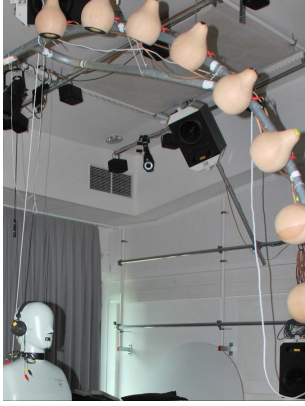


Fig. 3. Setup to measure $P(j\omega)$ and $S(j\omega)$: The loudspeakers are spaced every 12.5° from -75° to 87.5° on a vertical arc with 1.5 m radius. The headphones are put on a mannequin, which turns $12 \times 30^\circ$.

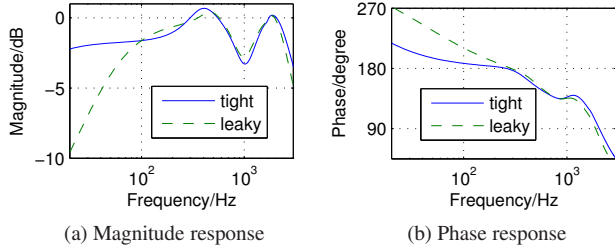


Fig. 4. Frequency response of $S(j\omega)$ for tight and leaky positioned headphones

4. PROTOTYPE FILTERS FOR THE ALC

4.1. PCA of the Required ANC Filters

The PCA changes the basis of a coordinate system with the goal to reduce the redundancy of dimensions for a given set of data. Its first principal component is the coordinate in which the data has the largest variance. The second principal component is orthogonal to the first and covers the largest remaining variance of the data, and so forth.

In our case, we want to change the basis of the matrix \mathbf{W} whose columns are the impulse responses \mathbf{w}_l of all measured variations of $\frac{P_l(j\omega)}{S_l(j\omega)}$. The secondary-path in the denominator is the transfer-function from the loudspeaker to the error microphone inside the ear-cup, and it is not minimum phase. Thus its inverse is acausal. The same applies to $P(j\omega)$ for those directions where the sound hits the error microphone earlier than the reference microphone. Since the acausal parts cannot be cancelled by the ALC, only the causal parts of \mathbf{w}_l are considered in \mathbf{W} .

The PCA transforms \mathbf{W} into a new matrix of impulse responses

$$\mathbf{H} = \mathbf{Q}_w^T \mathbf{W} \quad (3)$$

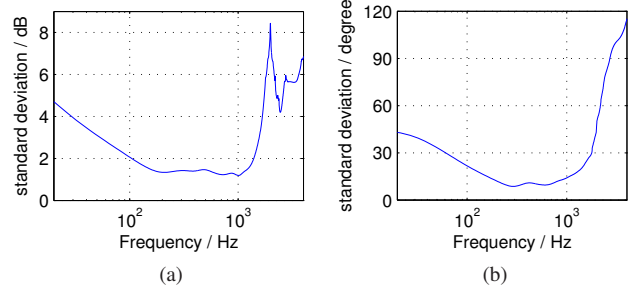


Fig. 5. Standard deviation of (a) magnitude and (b) phase of $P(j\omega)$ over all measurements.

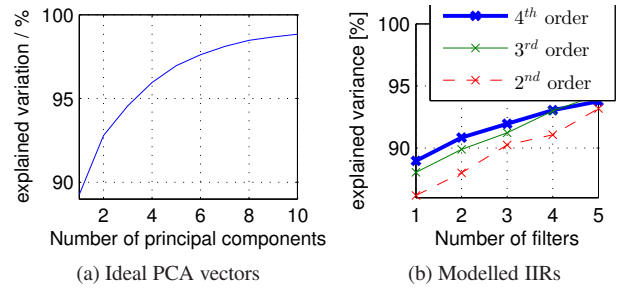


Fig. 6. Explained variance of the ideal PCA vectors (a), and the modelled IIR filters (b).

where the columns of \mathbf{Q}_w are the eigenvectors of $\mathbf{W}^T \mathbf{W}$. The corresponding eigenvalues λ_{w_i} are proportional to the variance that is explained by the corresponding principal component.

Fig. 6a shows that the amount of explained variation increases with the number of principal components. The impulse response \mathbf{h}_1 (i.e. the vector of \mathbf{H} corresponding to the largest eigenvalue) already models 89% of all required impulse responses with a scalable gain only, and four impulse responses would already model over 95%. The required transfer-functions $W_l(j\omega)$ are thus all very similar.

The resulting impulse responses \mathbf{h}_i could directly be implemented in the ALC as FIR filters. However, an IIR representation of the impulse responses is beneficial in order to reduce computational power and to allow for an analogue implementation of the system.

4.2. IIR Model of the Principal Component Filters

The numerator and denominator polynomials that model a given frequency response can be determined via the damped Gauss-Newton algorithm [9]. Due to the group delay of S , the impulse responses in \mathbf{W} and \mathbf{H} , respectively have an immediate onset. Furthermore, $P(j\omega)$ does not have sharp resonances and $S(j\omega)$ does not have sharp notches. Therefore a robustly stable IIR filter can be expected by the Gauss-Newton algorithm. The modelled IIR filters are only

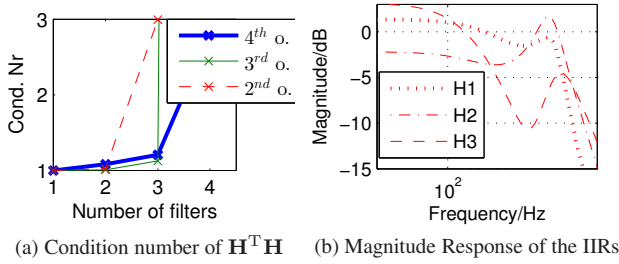


Fig. 7. Condition number dependent on filter number and order (a), and magnitude response of the three 3rd order filters (b).

approximations to the ideal transfer-functions from the PCA. The higher the IIR order, the closer is the approximation and the more variance of w_l can be explained.

The IIR filters are modelled with second, third, and fourth order and the explained variation is shown in Fig. 6b. Under the premise that the total order of the adaptive linear combiner should not be larger than 10, three 3rd order filters show the best results.

In addition, the three 3rd order filters are expected to yield a fast convergence because the condition number of $\mathbf{H}^T \mathbf{H}$ is small as can be seen in Fig. 7a. The magnitude response of the three chosen IIRs is shown in Fig. 7b.

5. RESULTS

The parallel IIR filters, with four numerator and three denominator coefficients each, require 21 multiplications and accumulations (MAC operations) per sampling interval. The secondary-path estimate \hat{S} can be modelled with three numerator and two denominator coefficients. Thus, the three filter operations with \hat{S} require another 15 MACs. With the three weight updates of the ALC, the complete system requires 39 MACs. This system is compared with an adaptive transversal-FIR filter that requires the same amount of MACs. The fxLMS of the transversal filter only requires one filter operation with \hat{S} , which consumes 5 MACs. That leaves 17 taps and 17 updates for the transversal filter.

5.1. Theoretical Results

The noise-cancelling error of the parallel IIR filters can be estimated as the difference between the measured variations \mathbf{W} and the adaptively combined IIRs:

$$\mathbf{E} = \mathbf{W} - \mathbf{H}\mathbf{G}, \quad (4)$$

where \mathbf{H} holds the three IIRs. The optimal weights can be derived over the least-squares solution

$$\mathbf{G} = (\mathbf{H}^T \mathbf{H})^{-1} \mathbf{H}^T \mathbf{W}. \quad (5)$$

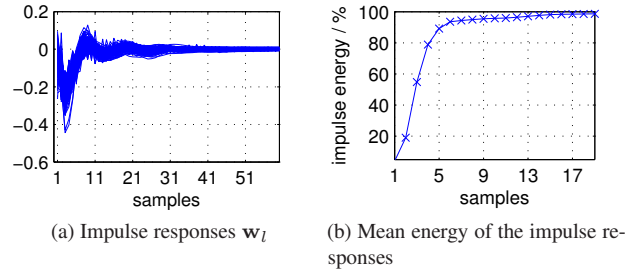


Fig. 8. Impulses responses (a) and percentage of the passed impulse-energy over time with a sampling frequency of 11025 Hz.

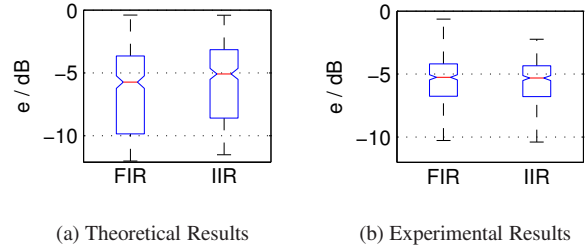


Fig. 9. Boxplot of estimated amount of residual noise.

To account for the sensitivity of the human ear, the optimization could be weighted with an A-weighting curve, but the above least-squares solution derives the minimum mean square error that can be achieved with the simple LMS algorithm.

The optimal solution of the transversal FIR are the first 17 samples of the impulse responses in \mathbf{W} that can be seen in Fig. 8a. At a sampling frequency of 11025 Hz, the 17 samples correspond to 1.5 ms. Fig. 8b shows that already 98% of the impulse energy has passed after 1.5 ms or 17 samples, respectively.

With the two above considerations, the noise-reduction of the two systems can readily be estimated. The residual error is set in relation to the reference x or w_l , respectively, and it is expressed in dB as

$$e_{\text{dB}} = 10 \log \frac{\sum_n e_l[n]^2}{\sum_n x[n]^2}, \quad (6)$$

Fig. 9a shows the distribution of e_{dB} over all $l = 1 \dots 336$ variations of w_l . It can be seen that there is hardly any difference in the optimum performance of the two systems.

The second performance criteria for adaptive noise control is the convergence speed that is bounded by the condition number of \mathbf{R} . Table 1 compares the condition number of both systems for white and pink noise. Both systems yield comparable condition numbers for white input noise. However for pink noise, the orthogonality of the three IIRs yields a far lower condition number than the autocorrelation matrix of the transversal FIR. A faster convergence of the three IIRs can

	3 IIRs	adapt. FIR
cond. white noise	1.1	1
cond. pink noise	20.0	60
λ_{\max} pink noise	210.0	590

Table 1. Condition number and λ_{\max} of \mathbf{R} .

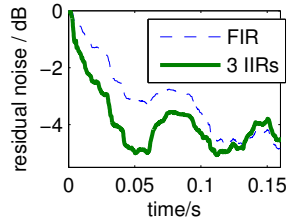


Fig. 10. Median residual noise over time.

thus be expected in real life applications because pink noise is a more realistic approximation of environmental noises than white noise.

5.2. Experimental Results

Both systems are tested with pink noise played back from all directions mentioned in section 3.1 with tight and leaky sitting headphones. In real-life applications, a predefined μ would be normalized by the input noise power because it is infeasible to constantly calculate the maximum eigenvalue of \mathbf{R} . This normalization would increase the complexity of the fxLMS, but the complexity would be equally increased for both systems under comparison. However, for the experiments, μ is still chosen according to $\frac{1}{2\lambda_{\max}}$ with the maximum eigenvalues given in Table 1 in order to be able to compare the results with the theoretical outcomes.

The distribution of the converged residual error over all directions is shown in Fig. 9b. The difference between the systems is even more balanced than in Fig. 9a.

In the second experiment, the transfer functions $\frac{P(j\omega)}{S(j\omega)}$ changed every 0.5 seconds, but this time, the weights \mathbf{g} were reset to zero before every change. Fig. 10 shows the median convergence behaviour from this zero vector to all measured transfer functions as median error e_{dB} over time. It confirms that the three parallel IIR filters converge faster than the transversal FIR.

6. CONCLUSION

In this work, suitable adaptive linear combiners are investigated for ANC headphones. The contributions of this paper are: (i) The investigation of the plant variation with consideration of different noise directions and different acoustic properties of the secondary-path. (ii) The deduction of parallel IIR prototype filters via PCA and based on the aforementioned

measurements. (iii) The comparison of the parallel IIR-ALC with a common adaptive transversal filter.

Restricted to a similar computation power, both systems perform equally well. However, the parallel ALC converges faster for coloured noise and requires less adaptation effort. This is especially beneficial if an analogue implementation of the adaptive system is desired. Analogue implementations are faster and less energy consuming, but they suffer from incorrect weight updates due to DC offsets in analogue active circuits [10]. Less adaptive weights therefore mean less effort to handle the DC offset.

REFERENCES

- [1] S.M. Kuo and D.R. Morgan, “Active noise control: a tutorial review,” *PIEEE*, vol. 87, no. 6, pp. 943–973, June 1999.
- [2] J.J. Shynk, “Adaptive iir filtering,” *ASSP Magazine, IEEE*, vol. 6, no. 2, pp. 4–21, 1989.
- [3] B. Bank, “Perceptually motivated audio equalization using fixed-pole parallel second-order filters,” *Signal Processing Letters, IEEE*, vol. 15, pp. 477–480, 2008.
- [4] G.A. Williamson and S. Zimmermann, “Globally convergent adaptive iir filters based on fixed pole locations,” *Signal Processing, IEEE Transactions on*, vol. 44, no. 6, pp. 1418–1427, 1996.
- [5] Jing Yuan, “Adaptive laguerre filters for active noise control,” *Applied Acoustics*, vol. 68, no. 1, pp. 86 – 96, 2007.
- [6] Jie Zeng and R. de Callafon, “Feedforward noise cancellation in an air duct using generalized fir filter estimation,” in *Decision and Control, 2003. Proceedings. 42nd IEEE Conference on*, 2003, vol. 6, pp. 6392–6397 Vol.6.
- [7] S.D. Snyder and C.H. Hansen, “The influence of transducer transfer functions and acoustic time delays on the implementation of the lms algorithm in active noise control systems,” *Journal of Sound and Vibration*, vol. 141, no. 3, pp. 409–424, 1990.
- [8] M. Guldenschuh, “Secondary-path models in adaptive-noise-control headphones,” in *Systems and Control (ICSC), 2013 3rd International Conference on*, Oct 2013, pp. 653–658.
- [9] J. E. Dennis, Jr. and Robert B. Schnabel, *Numerical Methods for Unconstrained Optimization and Nonlinear Equations (Classics in Applied Mathematics, 16)*, Soc for Industrial & Applied Math, 1996.
- [10] D.A. Johns, W.M. Snelgrove, and Adel S. Sedra, “Continuous-time lms adaptive recursive filters,” *Circuits and Systems, IEEE Transactions on*, vol. 38, no. 7, pp. 769–778, 1991.